

Exosomal linc-ROR mediates crosstalk between cancer cells and adipocytes to promote tumor growth in pancreatic cancer

Zhaowei Sun,^{1,2,8} Dong Sun,^{1,8} Yujie Feng,² Bingyuan Zhang,² Peng Sun,³ Bin Zhou,² Lutao Du,^{4,5,6} Yunshan Wang,^{4,5,6} Zhiyao Fan,¹ Jian Yang,¹ Yongzheng Li,¹ Sanyuan Hu,⁷ and Hanxiang Zhan¹

¹Division of Pancreatic Surgery, Department of General Surgery, Qilu Hospital, Cheeloo College of Medicine, Shandong University, Jinan, Shandong, China; ²Department of Hepatobiliary and Pancreatic Surgery, The Affiliated Hospital of Qingdao University, Qingdao, China; ³Department of Liver Transplant, The Affiliated Hospital of Qingdao University, Qingdao, China; ⁴Department of Clinical Laboratory, The Second Hospital, Cheeloo College of Medicine, Shandong University, Jinan, China; ⁵Shandong Engineering & Technology Research Center for Tumor Marker Detection, Jinan, China; ⁶Shandong Provincial Clinical Medicine Research Center for Clinical Laboratory, Jinan, China; ⁷Department of General Surgery, The First Affiliated Hospital of Shandong First Medical University, Jinan, China

Exosomes are emerging as important mediators of the crosstalk between tumor cells and stromal cells in the microenvironment. However, the underlying molecular mechanism of pancreatic cancer (PC)-derived exosomes in the progression of the tumor microenvironment (TME) and crosstalk with adipocytes has not been elucidated. Exosomes isolated from PC cell culture supernatant through ultracentrifugation were rich in long intergenic non-coding ROR (linc-ROR). After constructing PC cell lines with stable linc-ROR knockdown or overexpression via the transfection of short hairpin RNA (shRNA) and pLent-U6-GFP-Puro, direct and indirect coculture systems were established to simulate the interaction between adipocytes and PC cells. Next, the effects of conditioned medium collected from dedifferentiated adipocytes on PC cell proliferation, motility, metastasis, and epithelial-mesenchymal transition (EMT) were evaluated by western blot analysis, colony forming, real-time cell analysis (RTCA), 5-ethynyl-2'-deoxyuridine (EdU), immunofluorescence (IF), Transwell, and wound-healing assays *in vitro*. Xenograft models were employed to identify whether conditioned medium loaded with interleukin-1 β (IL-1 β) promoted PC cell growth *in vivo*. Our results demonstrate that linc-ROR delivery via exosomes represents a brand-new perspective of dedifferentiating adipocytes in the TME of PC, which further induce PC cell EMT via the hypoxia inducible factor 1 α (HIF1 α)-ZEB1 axis. Moreover, exosomal linc-ROR may become a novel diagnostic marker for PC patients.

INTRODUCTION

Pancreatic cancer (PC) is one of the most intractable carcinomas and is considered to have the worst prognosis among digestive system neoplasms.¹⁻³ Although different operative treatment options and adjuvant treatments, as well as neoadjuvant chemotherapy, are adopted to treat PC, the overall 5-year survival rate is still no more than 8%.⁴ The high mortality in patients with PC is primarily ascribed to

the lack of typical symptoms at its early stages and aggressive local invasion.⁵⁻⁷ Because current diagnostic tests are nonspecific, there is a necessity for exploring novel diagnostic biomarkers to gain a better comprehension of the molecular mechanisms underlying the origin and metastasis of PC.

Tumor development is not only determined by cancer cells but also regulated by hypoxia, lipids, and stromal cells in the tumor microenvironment (TME), three important factors involved in this process.⁸⁻¹⁰ Obesity is associated with an increased risk for several types of cancer, including PC, and increases the incidence and mortality of PC.^{11,12} Substantial evidence has shown that inflammation-related adipocytes in or around tumors promote oncogenesis.^{10,13} Moreover, obesity seems to alter the production of pro-inflammatory and chemoattractant chemokines. However, the mechanisms underlying adipocyte variation remain largely unknown in PC-related TME. Accordingly, exploring the relationship between adipocytes representing the obese environment and tumors is pressing.

Exosomes are double-layered extracellular vesicles (30–150 nm in diameter) that are secreted by diverse cell types, particularly tumor cells.¹⁴⁻¹⁶ They are considered extracellular messengers between tumor cells and the TME that communicate and exchange their abundant components, including long noncoding RNAs (lncRNAs).¹⁷⁻¹⁹ Our previous study confirmed that long intergenic non-coding ROR (linc-ROR) was highly upregulated in PC cells.²⁰ Another study also verified that exosomes secreted by tumor cells contribute to the progression of cancer by communicating with the surrounding

Received 11 November 2020; accepted 1 June 2021;
<https://doi.org/10.1016/j.omtn.2021.06.001>.

⁸These authors contributed equally

Correspondence: Hanxiang Zhan, Division of Pancreatic Surgery, Department of General Surgery, Qilu Hospital, Cheeloo College of Medicine, Shandong University, Jinan, Shandong 250012, China.

E-mail: zhanhanxiang@hotmail.com



stromal tissue.^{21,22} For instance, Takahashi et al.²³ confirmed that linc-ROR was highly expressed in extracellular RNA released by hepatocellular cancer (HCC) cells during hypoxia. He et al.²⁴ verified that exosomes derived from HepG2 cells reprogram the biological behaviors of LO2 cells by transferring linc-ROR, which influences recipient cells. Hardin et al.²⁵ illustrated the ability of exosomes to communicate with and modulate adjacent and distant tumor microenvironments through the transfer of linc-ROR and other modulators that also induce epithelial-mesenchymal transition (EMT).

More importantly, there are no relevant studies focusing on the relationship between adipocytes and exosomes derived from PC cells. To research the existence of crosstalk between adipocytes and PC cells and its consequences on the TME, we demonstrated that PC-cell-derived exosomes rich in linc-ROR expression could dedifferentiate adipocytes into fibroblast-like cells via a coculture system. The dedifferentiation of adipocytes leads to the intensive growth and metastatic potential of PC cells *in vitro* and *in vivo*. Additionally, exosomal linc-ROR acts as a clinical biomarker that is stable in serum and has the capacity to distinguish between someone who is carrying PC tumors or is healthy.

RESULTS

Characterization and role of exosomes related to linc-ROR derived from PC cells

To examine the influence of exosomes on adipocytes released from PC cells, exosomes were isolated from the supernatant (exosome-free serum of medium) and quantified by transmission electron microscopy (TEM) and nanoparticle tracking analysis (NTA). TEM showed clear rounded particles ranging from 30 to 150 nm in diameter (Figure 1A), and NTA exhibited a similar size distribution of exosomes (Figures 1B and 1C; Figure S1A) derived from PANC-1 and BxPC-3 cells. These results revealed that the exosomes were successfully isolated from the supernatant through ultracentrifugation. Next, higher expression of linc-ROR was observed in established PC cell lines (PANC-1, AsPC-1, MIA-PACA-2, CFPAC-1, and BxPC-3) compared to an immortalized normal pancreatic cell line (CCC-HPE-2) (Figure 1D). Moreover, differential expression of exosomal linc-ROR was consistent with intracellular linc-ROR (Figure 1E). However, we chose the PANC-1 and BxPC-3 cell lines for further research, since they exhibited the highest and lowest linc-ROR expression levels, respectively, compared to CCC-HPE-2. Western blot analysis of proteins extracted from exosomes isolated from CCC-HPE-2, PANC-1, and BxPC-3 cell supernatants demonstrated the existence of the exosomal proteins CD9 and TSG101 compared to the remainder supernatant (Figure 1F), as identified in the ExoCarta database (<https://bigd.big.ac.cn/databasecommons/database/id/580>).

Next, we investigated the stability of exosomal linc-ROR. Exosomes isolated from the supernatant of PANC-1 as a reference were cultivated with RNase A (10 µg/mL) for 0, 30, 60, and 90 min, and exosomal linc-ROR expression was measured at each time point (Figure 1G). As expected, expression levels of linc-ROR in exosomes

showed negligible changes upon RNase A digestion. Interestingly, the linc-ROR expression level in exosomes was conspicuously reduced (Figure S1B) when treated with RNase A and Triton X-100 together, suggesting that released linc-ROR was protected by a double-layer membrane instead of being directly discharged.

Furthermore, the ability of adipocytes to uptake PC cell exosomes was confirmed using confocal microscopy (Figures 1H and 2C; Figure S1C). As recipient cells, adipocytes showed uptake efficiency for exosomes from PC cells, suggesting that exosomal linc-ROR could be transmitted to adipocytes, indicating a promising role in regulating biological functions between PC cells and adipocytes.

Increased linc-ROR expression in exosomes derived from PC cells can be transferred to adipocytes, inducing dedifferentiation in a coculture system

It has been reported that exosomes contain several varieties of biologically active molecules, including lncRNAs, and that exosomal lncRNA bears a resemblance to that of the parent cells.^{26,27} We next examined the role of exosomal linc-ROR in inducing dedifferentiation of adipocytes using an *in vitro* indirect coculture model (Figure 2A). The coculture system separated adipocytes from PC cells by a 0.4 µm membrane through which exosomes could freely pass. Probing into the mechanisms of exosomal linc-ROR in the dedifferentiation of adipocytes, we proceeded with 5 days of induction of 3T3-L1 adipocytes that become mature adipocytes with distinctive lipid droplets (Figure 2B). The lipid droplets presented a regular round sphere by red oil staining. When isolated exosomes (green fluorescent dye, PKH67-labeled) derived from PC cells were cocultured with adipocytes, recipient cells (blue fluorescent dye, 4',6-diamidino-2-phenylindole [DAPI] labeled) expressed higher uptake potency as gauged by laser scanning confocal microscopy (LSCM) as time increased (Figure 2C; Figure S1C). This confirms that uptake capacity is time dependent.

To investigate how exosomal linc-ROR influences adipocytes through a coculture model, the plasmid vector short hairpin ROR (shROR) was used to knock down linc-ROR expression in PANC-1 cells. Adipocytes were maintained in a coculture system for 2 (post-induction day [PID] 7), 4 (PID 9), and 6 (PID 11) days after 5 (PID 5) days of induction. The same batch of adipocyte cells was cultivated independently and recorded at the same time points as the control. During coculturing with PANC-1 cells transfected with sh-negative control (CoshCtrl), mature adipocytes progressively exhibited considerable decreases in lipid droplets, and the cells became elongated in appearance, similar to a fibroblast-like morphology (Figure 2D), compared to transfection with shROR (CoshROR). Moreover, the morphological characteristics of adipocytes under the same experimental conditions were not distinctly altered at the different time levels between single adipocytes and the CoshROR group. In particular, the number of lipid droplets of adipocytes alone or in the CoshROR group was significantly increased on PID 11 compared to the CoshCtrl group of adipocytes after 6 days of coculture.

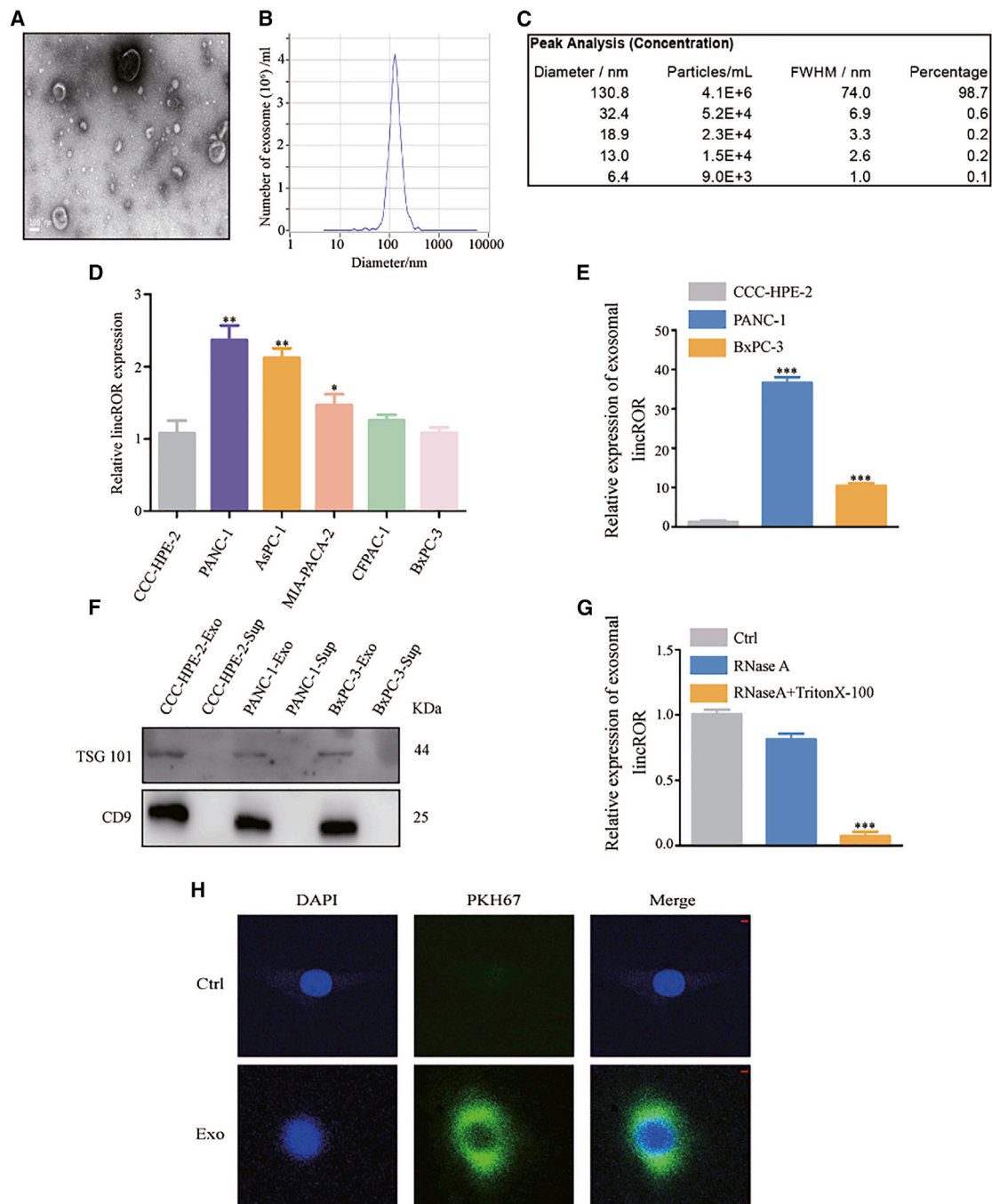
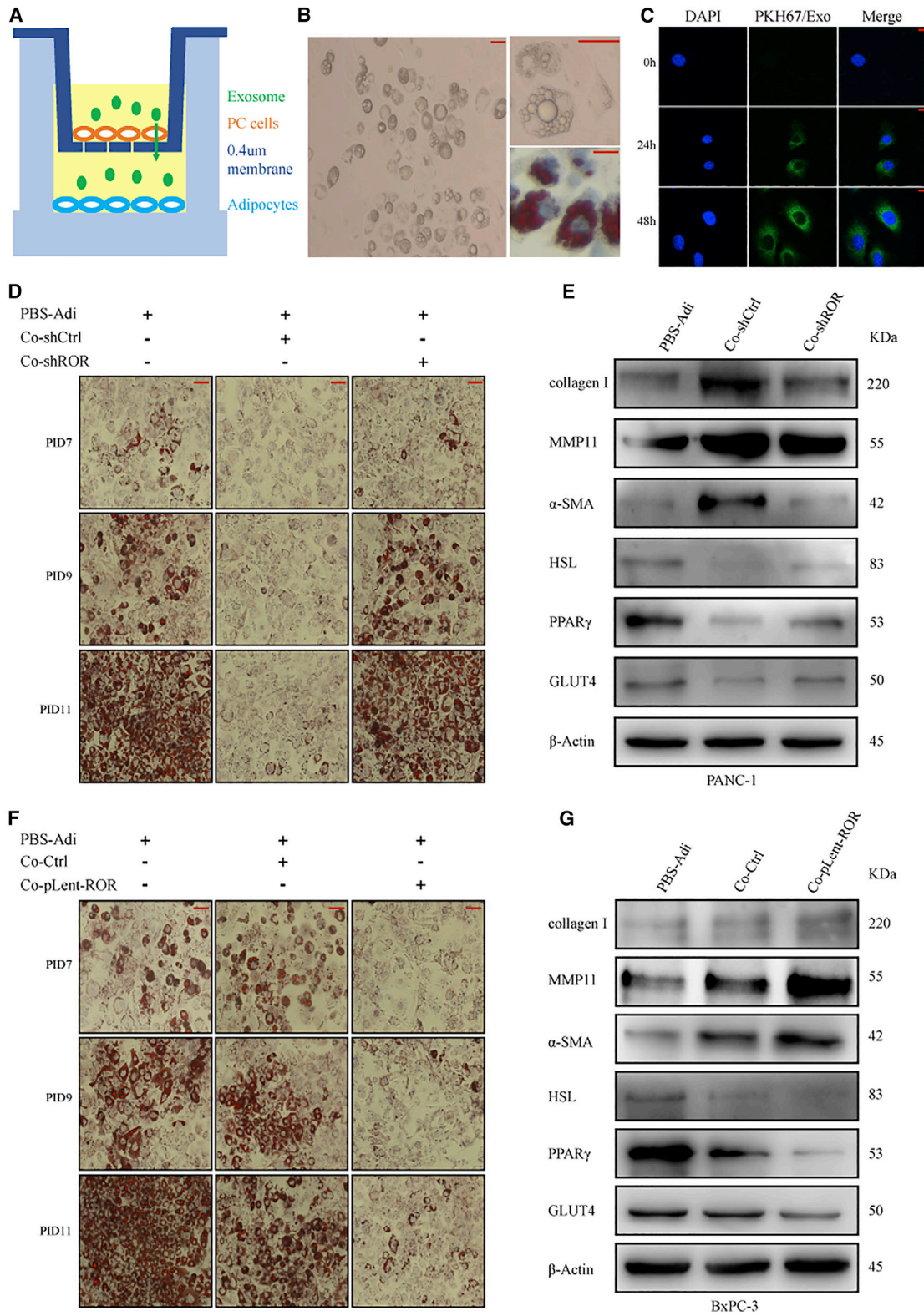


Figure 1. Characterization and roles of exosomes derived from PC cells

(A) Representative TEM image of the medium of PANC-1 cells as indicated by arrows. Scale bar, 100 nm. (B and C) Nanoparticle tracking analysis of the size distribution and number of exosomes derived from PANC-1 cells isolated by ultracentrifugation. (D) linc-ROR expression was measured in a normal pancreatic cell line (CCC-HPE-2) and in established PC cell lines (PANC-1, AsPC-1, MIA-PACA-2, CFPAC-1, and BxPC-3) using quantitative real-time PCR. (E) Quantitative real-time PCR analysis of linc-ROR expression in the exosomes of CCC-HPE-2, PANC-1, and BxPC-3 cells. (F) Western blotting analysis of CD9 and TSG101 in exosomes (Exo) and exosome-depleted supernatants (Sup) of CCC-HPE-2, PANC-1, and BxPC-3 cells. (G) Quantitative real-time PCR analysis of linc-ROR in exosomes treated or not with RNase A (10 μ g/mL) and/or 0.3% Triton X-100 and then further mixed with RNase inhibitor. (H) Internalization of exosomes (labeled with the membrane phospholipid dye PKH67) derived from PC cells. Scale bars, 10 μ m. Results are shown as the mean \pm SD. * p < 0.05, ** p < 0.01, *** p < 0.001.



(legend on next page)

To determine the mechanisms of exosomal linc-ROR in the induction of adipocyte dedifferentiation, we analyzed gene expression levels of adipocytes under different experimental conditions at PID 11 using western blot and quantitative real-time PCR. As expected, with respect to expression of some mature adipocyte-specific markers, such as glucose transporter-4 (GLUT4), proliferator-activated receptor gamma (PPAR γ), and hormone sensitive lipase (HSL), we observed a definite reduction in their expression levels of the CoshCtrl group compared to the CoshROR or single adipocyte (PBS-Adi) group (Figure 2E; Figure S1D, left). In addition, we detected expression levels of some fibroblast-specific genes, such as alpha smooth muscle actin (α -SMA), matrix metalloproteinase-11 (MMP11), and collagen I (Figure 2E; Figure S1D, right). Their expression levels notably increased after 6 days of coculture, further supporting the process of dedifferentiation of adipocytes toward fibroblast-like cells.

To better understand the role played by exosomal linc-ROR in the process of dedifferentiation, we implemented experiments using the plasmid vector pLent-ROR to overexpress linc-ROR. Conversely, coculture with linc-ROR-overexpressing BxPC-3 cells (CopLent-ROR) significantly inhibited protein and mRNA levels of mature adipocyte-specific markers compared to BxPC-3 cells treated with pLent-negative control in a coculture system (Co-Ctrl) or single adipocytes (Figure 2G; Figure S1E, left). The micromorphology of adipocytes was identical to that of PANC-1 cells under the same experimental conditions (Figure 2F). CopLent-ROR of adipocytes still presented higher fibroblast-specific genes at PID 11 compared to Co-Ctrl or single adipocytes assayed by western blot and quantitative real-time PCR, as previously observed in the PANC-1 cell coculture system (Figure 2G; Figure S1E, right). According to the above results, using a coculture system we substantiated that PC tumor-derived exosomal linc-ROR promotes the dedifferentiation of adipocytes.

Adipocytes dedifferentiated via exosomal linc-ROR promote PC tumorigenesis

After exploring the effect of exosomal linc-ROR on the induction of adipocytes dedifferentiated using a coculture system, we next examined the effects of conditioned medium collected from adipocytes treated with different types of exosomes derived from linc-ROR overexpression/knockdown or negative control PANC-1 and BxPC-3 cells on PC cell biological behaviors. Combining previous studies,¹⁰ in order to isolate the role of linc-ROR from PC cells acting on themselves, we adopted a direct coculture model rather than an indirect model by adding exosomes into adipocyte medium through an indirect coculture system followed by using the newly acquired conditioned medium to directly stimulate PC cells. By analyzing the conditioned medium's effects from multiple cell proliferation assays in PC cells, as

expected, we found that the conditioned medium effectively promoted growth in PANC-1 and BxPC-3 cells. We compared the reproductive capacity of three groups of PC cells—PBS-shCtrl, CoshCtrl, and CoshROR—in PANC-1 cells and PBS-pLent-ROR, Co-Ctrl, and CopLent-ROR in BxPC-3 cells. Functionally, the results of colony-formation assays showed that the knockdown/overexpression of exosomal linc-ROR expression in the coculture system significantly reduced/potentiated PC cell growth viability (Figures 3A and 3B), and the real-time cell analysis (RTCA) xCELLigence experiments produced analogous results (Figures 3C and 3D). As shown in the figure panels, the coculture/higher linc-ROR group exhibited improved growth compared to their respective control groups. These results were also confirmed by further 5-ethynyl-2'-deoxyuridine (EdU) experimental results (Figures 3G and 3H). Based on the above results, the dedifferentiation of adipocytes with higher exosomal linc-ROR expression increases the proliferation ability of PC cells.

A coculture system between adipocytes and PC cells induces migration, invasion, and morphological alteration of PC cells accompanied by EMT

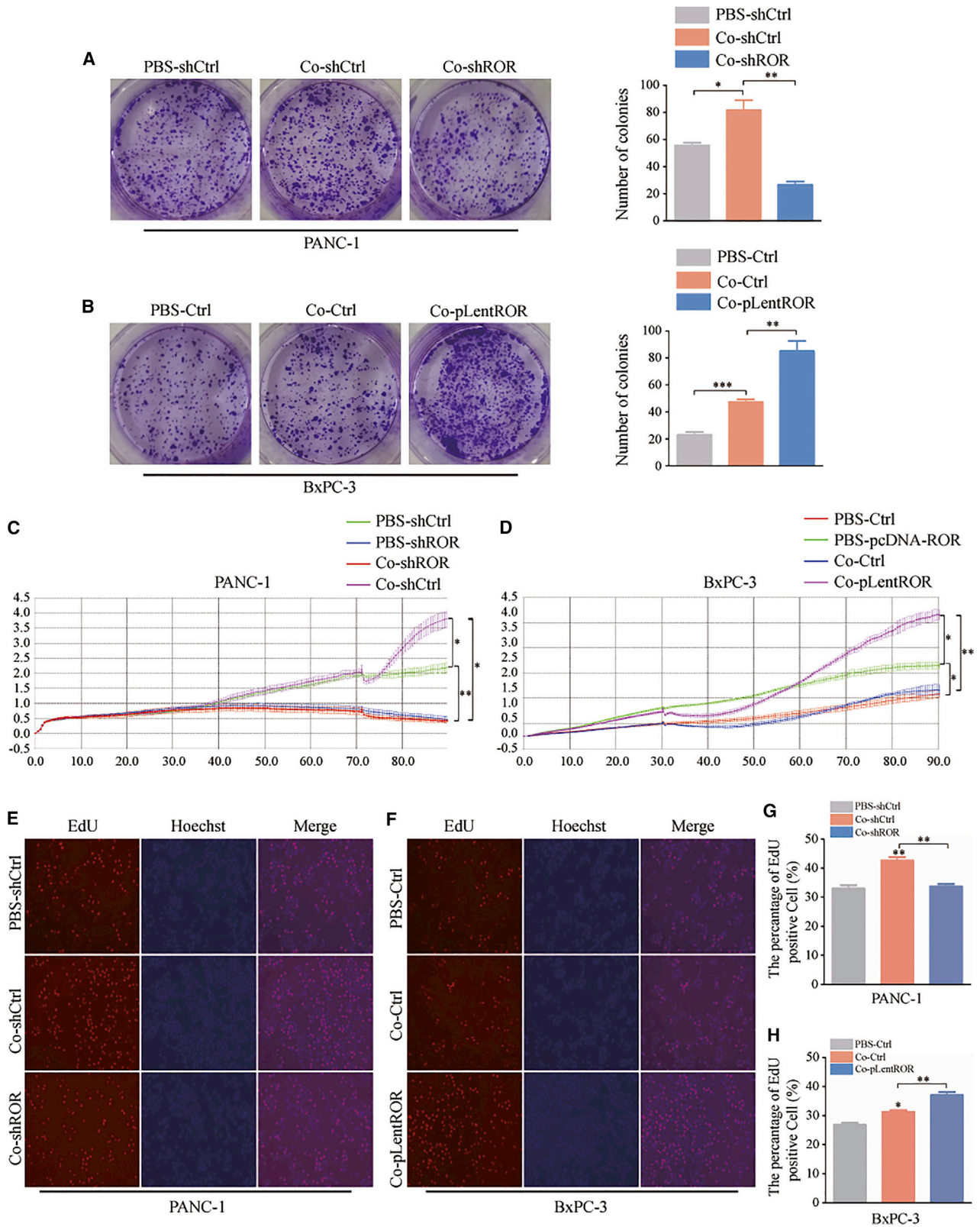
Our findings also showed that conditioned medium of the coculture system between adipocytes and exosomal linc-ROR enhanced the motility of PC cell lines compared to PBS-shCtrl/PBS-Ctrl (Figures 4A and 4B). Importantly, we found that dedifferentiation of adipocytes induced by increased exosomal linc-ROR expression made PC cells more capable of motion as shown by wound-healing assays (Figures 4A and 4B). Furthermore, conditioned medium generated from adipocytes processed with exosomal linc-ROR, to a great degree, induced migration and invasion of PC cells across Transwell filters (Figures 4C and 4F). The images also showed that conditioned medium altered the morphology of PC cells from the condensed type into the dispersed type (Figure 5B), typified by lost intercellular junctions and extended cellular pseudopods, accompanied by increased expression of the mesenchymal marker vimentin and decreased expression of the epithelial marker E-cadherin as shown through immunofluorescence (IF) assay (Figure 5A). Conversely, increasing linc-ROR expression in BxPC-3 cell exosomes magnified these effects (Figures S2A and S2B). These data confirmed that increasing expression of exosomal linc-ROR, which acts on adipocytes via a coculture system, promotes PC metastasis *in vitro*.

Exosomal linc-ROR induces dedifferentiation of adipocytes and facilitates EMT in PC cells by activating the HIF1 α /ZEB1 signaling pathway and interleukin-1 β (IL-1 β)

We next thoroughly investigated the biological function of exosomal linc-ROR and conditioned medium of adipocytes in the PC microenvironment. To examine the crosstalk between adipocytes and PC

Figure 2. Increased levels of linc-ROR expression in exosomes derived from PC cells can be transferred to adipocytes and induce dedifferentiation through the coculture system

(A) Schematic illustration of the *in vitro* indirect coculture system. (B) Representative microscopy image of typical lipid vacuoles of adipocytes alone or using red oil staining. Scale bars, 20 μ m. (C) Labeled PC-Exos (green fluorescent dye, PKH67) were taken up by adipocytes (blue fluorescent dye, DAPI) for 0, 24, and 48 h. Scale bars, 10 μ m. (D and F) Cocultured adipocytes with exosomal linc-ROR presented a progressive reduction in area and number compared to controls for PID 7, 9, and 11. Scale bars, 20 μ m. (E and G) Western blot data showing expression of mature adipose-specific genes and fibroblast-specific markers.



(legend on next page)

cells, we analyzed hypoxia inducible factor 1 α (HIF1 α) expression in PANC-1 cells transfected with shCtrl when cocultured with adipocytes compared to cells not cocultured (PBS was a negative control) or cocultured with PANC-1 cells transfected with shROR at different times. As shown in Figure 6A, only adipocytes treated with increased exosomal linc-ROR exhibited dedifferentiation, ultimately promoting HIF1 α expression with the extension of coculture time (0 h, 24 h, and 48 h). In addition, we measured expression of ZEB1 in PANC-1 cells cocultured with adipocytes (Figure 6B). Results showed that adipocytes not only promote HIF1 α expression but also promote expression of ZEB1 over time in coculture. HIF1 α played a central role in effective restructuring of the ZEB1 signaling pathway during the coculture system. We used quantitative real-time PCR and western blotting to investigate whether HIF1 α activates the ZEB1 pathway in coculture condition compared to PBS as a control (Figure 6C; Figures S1A left, S1B, and S1C). As expected, the decrease in HIF1 α induced by small interfering RNA (siRNA) (si-HIF1 α) reduced ZEB1 expression. In particular, the HIF-1 α and coculture model had a synergistic positive regulatory effect on ZEB1 (Figure 6I). Functionally, colony-formation and EdU assays were used to detect whether HIF1 α influenced PANC-1 cell proliferation (Figures S1G and S1H). Additionally, both wound-healing and Transwell assays revealed that loss of HIF1 α in PANC-1 cells reduced their migration and invasion abilities (Figures S1D and S2B). Altogether, these results indicate that HIF1 α mediates growth, invasion, and metastatic alterations through the ZEB1 pathway in PC cells.

To increase the rigor of the above results, BxPC-3 cells transfected with pLent-ROR were used to explore whether overexpression of linc-ROR causes alterations in downstream HIF1 α -ZEB1 expression. Experimental results revealed the efficiency and feasibility of linc-ROR and coculture conditions in the HIF1 α -ZEB1 signaling pathway compared to BxPC-3 cells treated with pLent-negative control or PBS-Ctrl over time (Figures 6D–6F; Figure S1A, right). Based on our previous review, we proceeded with the inductive reasoning that cytokines, such as IL-1 β , play important mediating roles between adipocytes and tumor cells through paracrine signaling in the PC microenvironment.¹⁰ Therefore, we also assessed IL-1 β concentrations in the coculture microenvironment with adipocytes through ELISA (Figures 6G and 6H). The data revealed that higher exosomal linc-ROR provokes adipocytes to secrete IL-1 β .

In addition, western blot analysis of PC cells revealed typical changes in cells with ZEB1-induced EMT, including decreased E-cadherin protein expression but dramatically increased vimentin (Figures 6C, 6F, and 6I; Figure S1A). Therefore, these results demonstrated that exosomal linc-ROR induces dedifferentiation of adipocytes and enhances expression of ZEB1 in PC cells, which induces EMT.

The tumor microenvironment mediated by exosomal linc-ROR facilitates tumor growth of PC cells via conditioned medium collected from adipocytes *in vivo*

To further evaluate the function of exosomal linc-ROR in the transforming phenotype of adipocytes, which stimulates the progression of PC proliferation *in vivo*, BxPC-3 cells mixed with the conditioned medium of adipocytes stimulated by exosomes derived from BxPC-3-shCtrl (PBS-Ctrl and Co-Ctrl) or transfected with pLent-ROR (PBS-pLent-ROR and CopLent-ROR) were subcutaneously inoculated into nude mice (Figure 7A). Importantly, intratumor injection of conditioned medium (three times a week) from dedifferentiated adipocytes treated with overexpressed exosomal linc-ROR resulted in the largest tumor growth volume at different points in time (Figure 7B). After 5 weeks, we observed that BxPC-3 cells mixed with CopLent-ROR exhibited larger tumor nodules than those generated by BxPC-3 cells alone (Co-Ctrl) or those mixed with PBS-Ctrl (Figure 7C). Moreover, expression of Ki-67 protein in the PBS-Ctrl or PBS-pLent-ROR group was significantly lower than in the Co-Ctrl and CopLent-ROR groups (Figure 7D). These results indicate that exosomal linc-ROR in the TME induces adipocyte dedifferentiation to facilitate PC growth *in vivo*.

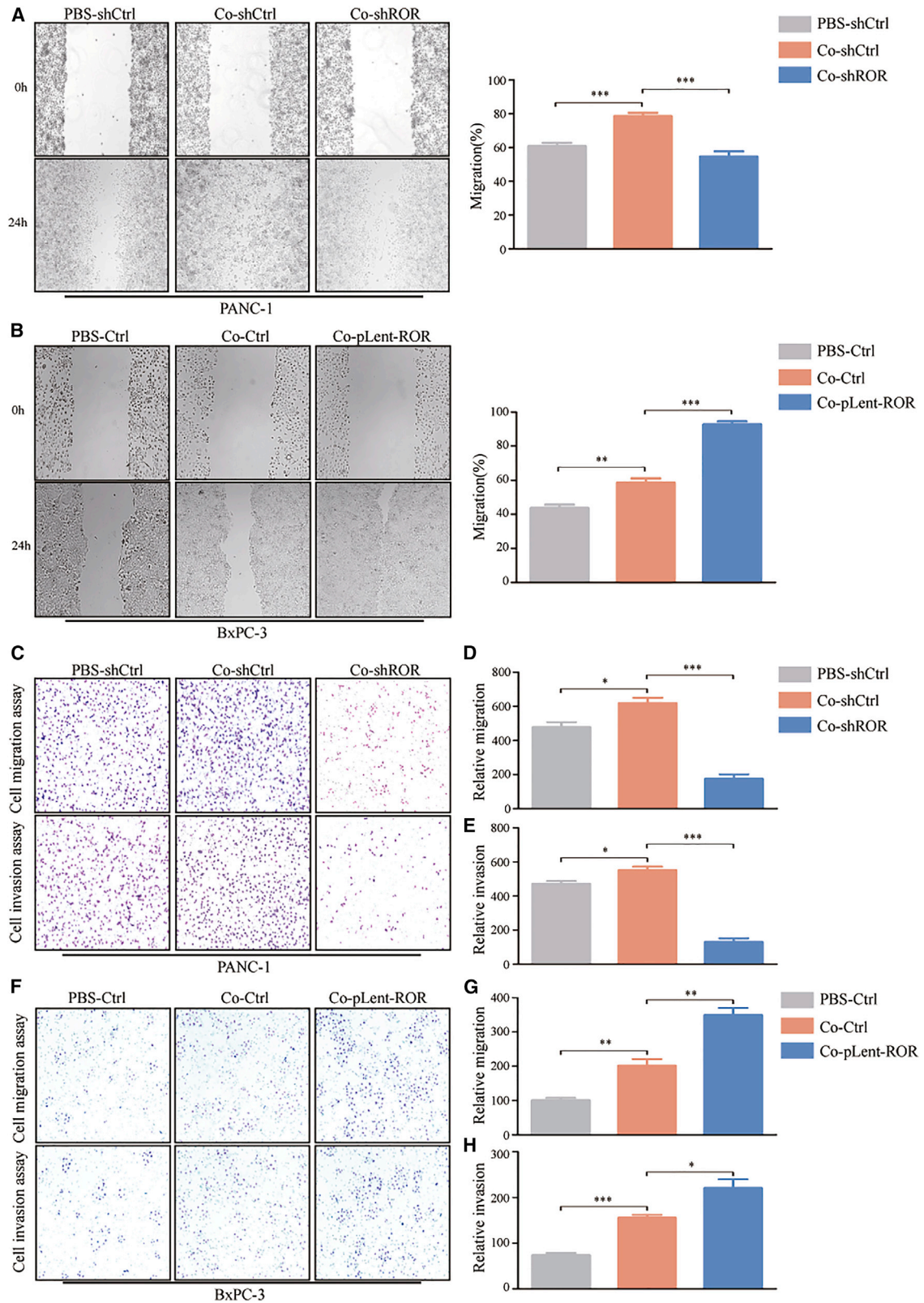
Meanwhile, previous exosome characterization studies have indicated that linc-ROR encapsulated in exosomes has better stability under the protection of the membrane (Figures 1G and 1H), which is an essential prerequisite for good biomarkers. Taken together, to validate the diagnostic performance of exosomal linc-ROR in serum, its expression was measured in the same validation cohort (Figure 7E). Moreover, receiver operator characteristic (ROC) curve analysis was performed according to the expression of exosomal linc-ROR in 48 PC patients and 48 healthy individuals (Figure 7F). As expected, the area under ROC curve (AUC) of exosomal linc-ROR for PC detection was 0.854 (95% confidence interval = 0.767–0.918). The best cut-off value of serum exosomal linc-ROR for predicting PC was 1.21086 (fold change in CRC compared to healthy individuals), with a sensitivity of 72.92% and a specificity of 95.83%, suggesting that exosomal linc-ROR is a promising serum biomarker for the diagnosis of PC.

DISCUSSION

Hypoxia and inflammation exist in all solid tumors and are associated with tumor angiogenesis, glycolysis, growth factor signaling, aggressive phenotypes, and poor prognosis.^{28,29} On the one hand, HIF1 α , which is stabilized under conditions of hypoxia³⁰ and leads to enhanced migration and invasion by the HIF1 α -ZEB1 axis,³¹ plays a pivotal role in the function of the tumor microenvironment.³² On the other hand, inflammation can be induced by obesity in PC, which is also associated with increased tumor growth and metastasis.^{13,33} Exosomes are lipid bilayer-enclosed extracellular vesicles that contain

Figure 3. Adipocytes dedifferentiated via exosomal linc-ROR promote PC tumorigenesis

(A) Colony-formation ability of PANC-1 cells treated with PBS-shCtrl, CoshCtrl, and CoshROR was determined by colony-formation assays. (B) Colony-formation ability of BxPC-3 cells treated with PBS-Ctrl, Co-Ctrl, and CopLent-ROR was determined by colony-formation assays. (C and D) The xCELLigence system was used to monitor the cell growth dynamics with real-time cell analysis (RTCA) of different groups of PC cells. (E–H) An EdU assay was performed to determine the proliferation of different groups of PC cells.



(legend on next page)

different types of proteins and nucleic acids, particularly lncRNAs. Here, we purified exosomes from the supernatant of PANC-1 and BxPC-3 cells and explored the role and underlying mechanisms of exosomal linc-ROR in the progression of PC.

We found that PC cells released increased levels of exosomal linc-ROR into the circulating system compared with the normal pancreatic cell line (CCC-HPE-2), with good stability from membrane protection and the overexpression of serum-derived exosomal linc-ROR in patients with PC, suggesting that exosomal linc-ROR may function as an oncogene in PC and may represent a marker of cancer occurrence. Exosomes are released by various cells, especially tumor cells, and circulate in the blood of cancer patients, potentially correlating with the biological behaviors of tumor progression.^{34–36} Recently, accumulating evidence has indicated that exosomes can transfer bioactive molecules between recipient cells and cancer cells in local and distant microenvironments. Deng et al.³⁷ confirmed that lncRNA CCAL transferred from fibroblasts by exosomes promotes chemoresistance of colorectal cancer cells. Wang et al.³⁸ also demonstrated that exosome-encapsulated microRNAs (miRNAs) contribute to liver metastasis in colorectal cancer by enhancing M2 polarization of macrophages. It is well known that the PC microenvironment contains abundant stromal cells, including cancer-associated adipocytes (CAAs), cancer-associated fibroblasts (CAFs), tumor-associated macrophages (TAMs), and endothelial cells.^{9,39,40} Combining our previous review about obesity and PC in 2019,⁴¹ however, the molecular mechanism between these cell types remains unclear. In this study, we demonstrated an interaction between adipocytes in an obesity model and PC cells using a cellular and molecular perspective. Using an indirect coculture model, we constructed a situation in which PC cells affected adipocytes through exosomes, which functionally changed their maturation and resulted in dedifferentiation of 3T3-L1 adipocytes, leading to loss of the adipocyte-specific gene expression profile (GLUT4, HSL, and PPAR γ) and acquisition of reprogrammed gene expression (MMP11, collagen I, and α -SMA). Adipocytes can act on other cells, especially cancer cells in the TME, via different pathways. For instance, adipocytes can induce EMT, which promotes breast cancer cells to acquire an aggressive tumor phenotype.⁴² More importantly, Incio et al.¹³ confirmed that obesity induced inflammation and desmoplasia in a transgenic mouse model of pancreatic ductal adenocarcinoma (PDAC), in which IL-1 β is released by adipocytes. The cell culture media from adipocytes increased the invasive ability and EMT gene expression of B16BL6 melanoma cells.⁴³ In this study, we found that culture medium from adipocytes treated with excess exosomal linc-ROR via a direct coculture model released increased IL-1 β levels. Furthermore, our results also revealed that conditioned culture medium collected from adipocytes gives rise to the characteristic morphological change

observed in PC cells, which was followed by increased migration, invasion, and EMT *in vitro* and proliferation both *ex vivo* and *in vivo*. These results suggest that PC-cell-derived exosomal linc-ROR plays a crucial role in the TME interactions between adipocytes and PC cells and is important for tumor growth and spread.

The cytokine IL-1 β is necessary for the host response and resistance to pathogens and exacerbates damage from chronic disease and acute tissue injury, which are pivotal mediators of the inflammatory response.^{44,45} Moreover, our previous review showed that IL-1 β and IL-6 led to local tissue fibrosis, which plays important roles in the bidirectional crosstalk between adipocytes and PC cells through paracrine signaling.⁴¹ There are also relevant studies confirming that the synthesis of HIF1 α is upregulated by increasing IL-1 β in HCC cells through cyclooxygenase-2⁴⁶ and IL-6 in hemangioma cells via activation of VEGFA signaling.⁴⁷

In the present study, after measuring concentrations of IL-1 β derived from adipocytes with or without exosome coculture, we found that high doses of IL-1 β have the ability to magnify the effects of cell growth and metastasis accompanied by EMT in PC compared to low doses. Next, we discovered that expression of HIF1 α was increased by conditioned culture medium that was particularly rich in IL-1 β . Furthermore, it is important to note that these processes in PC cells are molecularly linked by HIF1 α , and multiple studies have confirmed that HIF1 α promotes EMT through direct regulation of ZEB1 expression, such as in glioblastoma,³¹ colorectal cancer,⁴⁸ and bladder cancer.⁴⁹ Given the enhanced growth and metastatic capacities of PC cells, our current study found that the increased HIF1 α expression induced by IL-1 β in conditioned medium resulted in activation of the ZEB1 signaling pathway. Unexpectedly, knockdown of HIF1 α not only reduced expression of ZEB1 but also blocked the effect of coculturing with conditioned medium on EMT to a great extent. Accordingly, these data suggest that HIF1 α plays an important role in the metastasis of PC.

Our findings demonstrate that exosomal linc-ROR not only acts as a clinical biomarker of PC but also mediates crosstalk between PC cells and adipocytes in TME. After exposure to exosomes, activated adipocytes may dedifferentiate into preadipocyte/fibroblast-like cells by releasing the cytokine IL-1 β , which in turn sustains PC cell growth and metastasis via the HIF1 α -ZEB1 axis (Figure 8).

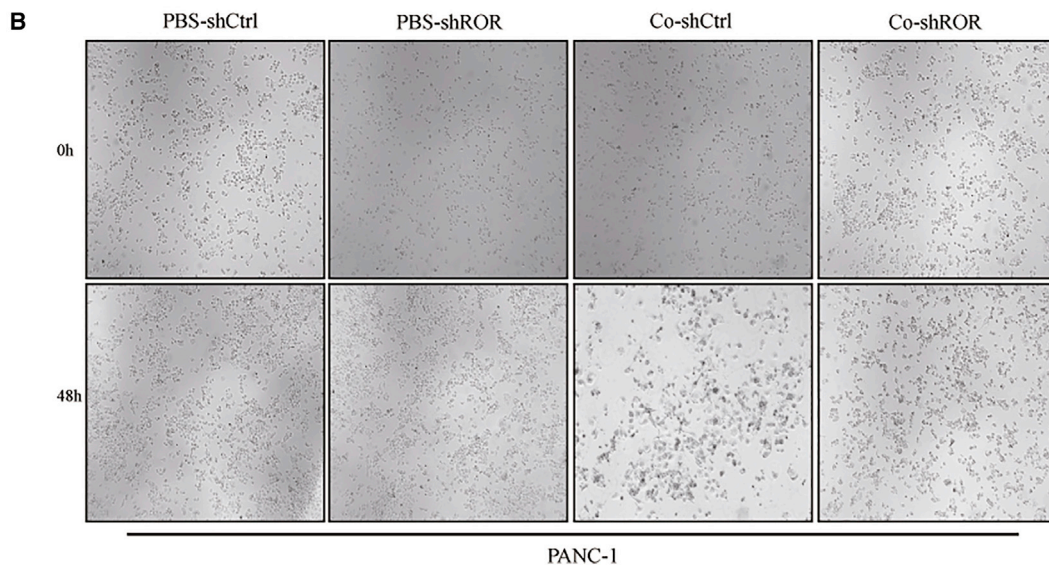
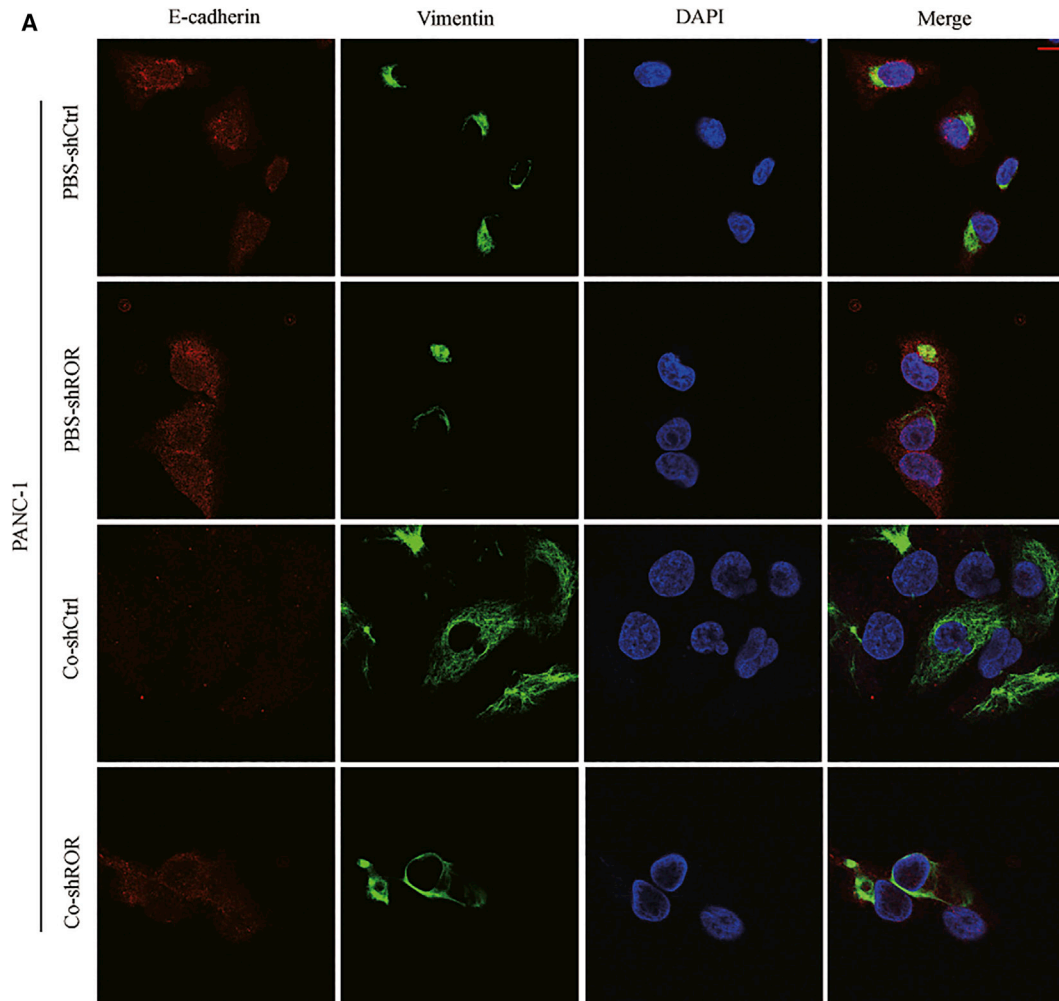
MATERIALS AND METHODS

Clinical PC serum samples

All serum samples were drawn from Qilu Hospital and The Second Hospital of Cheeloo College of Medicine, Shandong University between December 2017 and January 2020, and informed consent

Figure 4. A coculture system between adipocytes and PC cells induces migration and invasion

(A) Motility of PANC-1 cells treated with PBS-shCtrl, CoshCtrl, and CoshROR assessed by wound-healing assays. (B) Motility of BxPC-3 cells treated with PBS-Ctrl, Co-Ctrl, and CopLent-ROR was assessed by wound-healing assays. (C–E) The effect of PANC-1 cells treated with PBS-shCtrl, CoshCtrl, and CoshROR on migration and invasion was determined by the Transwell assay. (F–H) The effect of BxPC-3 cell treatment with PBS-Ctrl, Co-Ctrl, and CopLent-ROR on migration and invasion was determined by the Transwell assay.



(legend on next page)

was obtained from all participants. A total of 96 peripheral blood samples were collected by medical professionals, including 48 patients with PC and 48 healthy controls who did not receive any surgical resections or pharmacological interventions before sample collection. All PC patients were diagnosed by biopsy or histopathology. First, all samples were collected within 2h in coagulation-promoting vacuum tubes and were sequentially isolated following a two-step centrifugation ($1,200 \times g$ for 5 min and $9,600 \times g$ for 5 min at 4°C) to remove cell sediments. Subsequently, total supernatants of two types of samples were transferred into 1.5 mL RNase- and DNase-free Eppendorf tubes and stored at -80°C until further analysis. This study was approved by the Ethics Committee of Qilu hospital, Cheeloo College of Medicine, Shandong University and was conducted in accordance with ethical principles of the World Medical Association and the Declaration of Helsinki.

Cell culture

Normal pancreatic cells (CCC-HPE-2), five established PC cell lines (PANC-1, AsPC-1, MIA-PACA-2, CFPAC-1, and BxPC-3), HEK293T, and 3T3-L1 cells were obtained from ATCC. 3T3-L1 cells were cultured in DMEM supplemented with 10% newborn calf serum (NBS), and other cell lines were cultured in DMEM supplemented with 10% fetal bovine serum (FBS) at 37°C in an incubator with 5% CO_2 . At 50%–70% confluence, 3T3-L1 cells cultured in DMEM with 10% NBS were detached by trypsin-EDTA solution with phenol red (Gibco) and were seeded into 6-well plates (Corning) containing a slide with an attached Transwell chamber ($0.44 \mu\text{m}$ pore size; Corning). After the cells overgrew on the bottom wall of the 6-well plates, they were induced to differentiate in DMEM containing 10% FBS replacing NBS, 0.2 mM IBMX (Sigma), 1 μM dexamethasone (Sigma), and 10 $\mu\text{g}/\text{mL}$ insulin (Sigma) for 2 days. After PID 2, the medium was replaced with DMEM containing 10% FBS and 10 $\mu\text{g}/\text{mL}$ insulin, and cells were cultured for another 2 days (PID 4). Then, cells were cultured in 10% FBS medium containing new insulin for another day (PID 5). Five days after adipocyte induction, cells were cocultured with PC cells using a Transwell system as an indirect coculture model in new medium without insulin. Different types of transfected PC cells were seeded into the top chamber. The coculture medium was replaced twice, and 3T3-L1 cells were cocultured with PC cells for an additional 2 days (PID 7), 4 days (PID 9), and 6 days (PID11). All types of PC cells and induced adipocytes were also cultured individually as a negative control (NC) and directly evaluated at the same time points. Oil Red O staining (Solarbio) was used to stain lipids of adipocytes according to the manufacturer's instructions.

Purification and identification of exosomes

Exosomes were purified from the serum and supernatants of CCC-HPE-2, PANC-1, and BxPC-3 cells by $0.22 \mu\text{m}$ filtration (Merck Millipore) and ultracentrifugation (Beckman Coulter) as we previ-

ously described.⁵⁰ Then, the surface morphology and ultrastructure of exosomes from PANC-1 and BxPC-3 cell supernatants were analyzed by means of TEM. NTA was performed to calculate exosome size distribution using Zetaview (Particle Metrix) equipped with fast video capture according to the manufacturer's instructions. In addition, exosome-specific proteins (CD9 and TSG101) were identified using western blotting.

Exosome labeling and tracking

PKH67 Green Fluorescent membrane linker dye (Sigma-Aldrich) was used to label purified exosomes isolated from PC cell supernatants according to the manufacturer's instructions. Next, the traced exosomes were resuspended and added to the adipocyte medium for exosome uptake studies using an indirect coculture model. After coculturing for 0 h, 24 h, and 48 h at 37°C with 5% CO_2 , DAPI (Invitrogen) was used for adipocyte nuclear staining. Finally, the glass slides were fluorescently visualized using an Axio-Imager-LSM800 laser scanning microscope (ZEISS).

Lentivirus production and cell transfection

Both lentivirus-containing shRNA and the pLent3.1 vector targeting linc-ROR were purchased from Genechem. Forty-eight hours post transfection, cells were sifted with puromycin for 6 days to construct different types of cell lines with stable linc-ROR knockdown or over-expression. siRNA/si-negative control (si-NC) of HIF1 α (si-HIF1 α) was purchased from GenePharma. PC cells were transfected with siRNAs using Lipofectamine 2000 (Invitrogen) according to the manufacturer's instructions.

Quantitative real-time PCR analysis and primers

Total RNA was extracted from PC and adipocyte cells and exosomes of serum and cell culture supernatant via TRIzol Reagent (Invitrogen). RNA was reverse transcribed using random primers under the standard conditions for the Prime Script RT reagent Kit (TaKara). SYBR Premix Ex Taq (TaKara) was used to analyze real-time PCR. RNA input was normalized to the level of GAPDH. The primer sequences used were as follows: GAPDH primers, forward: 5'-GCACCGTCAAGGCTGAGAAC-3', reverse: 5'-TGGTGAAGACGCCAGTGGA-3'; linc-ROR primers, forward: 5'-TCTTAGCAGGCATTTTGGAGG-3', reverse: 5'-GAAGCAGAATGCAGGATGGT-3'; ZEB1 primers, forward: 5'-CGCAGTCTGGGTGTAATCGT-3', reverse: 5'-TGTTCTTGGTCGCCATTCA-3'; HIF1 α primers, forward: 5'-GAACGTCGAAAAGAAAAGTCTCG-3', reverse: 5'-CCTTATCAAGATGCGAACTCACA-3'; MMP11 primers, forward: 5'-TGTGAGACTTCCTTCGACGC-3', reverse: 5'-AGAACCAAA TCTGGCCCTGG-3'; collagen I primers, forward: 5'-ACGCCATC AAGGTCTACTGC-3', reverse: 5'-ACTCGAACGGGAATCCATC G-3'; α -SMA primers, forward: 5'-GCTGGACTCTGGAGATGG TG-3', reverse: 5'-CAATCTCACGCTCGGCAGTA-3'; GLUT4

Figure 5. The coculture system altered the morphology of PANC-1 cells and induced EMT

(A) Representative images of IF micrographs of the subcellular localization and expression of E-cadherin (red) and vimentin (green) in PANC-1 cells treated with PBS-shCtrl, PBS-shROR, CoshCtrl, and CoshROR for 48 h. Nuclei were counterstained with DAPI (blue). Scale bars, 50 μm . (B) The morphology of PANC-1 cells incubated with conditioned medium of adipocytes cocultured with PBS-shCtrl, PBS-shROR, CoshCtrl, and CoshROR of PANC-1 cells for 48 h.

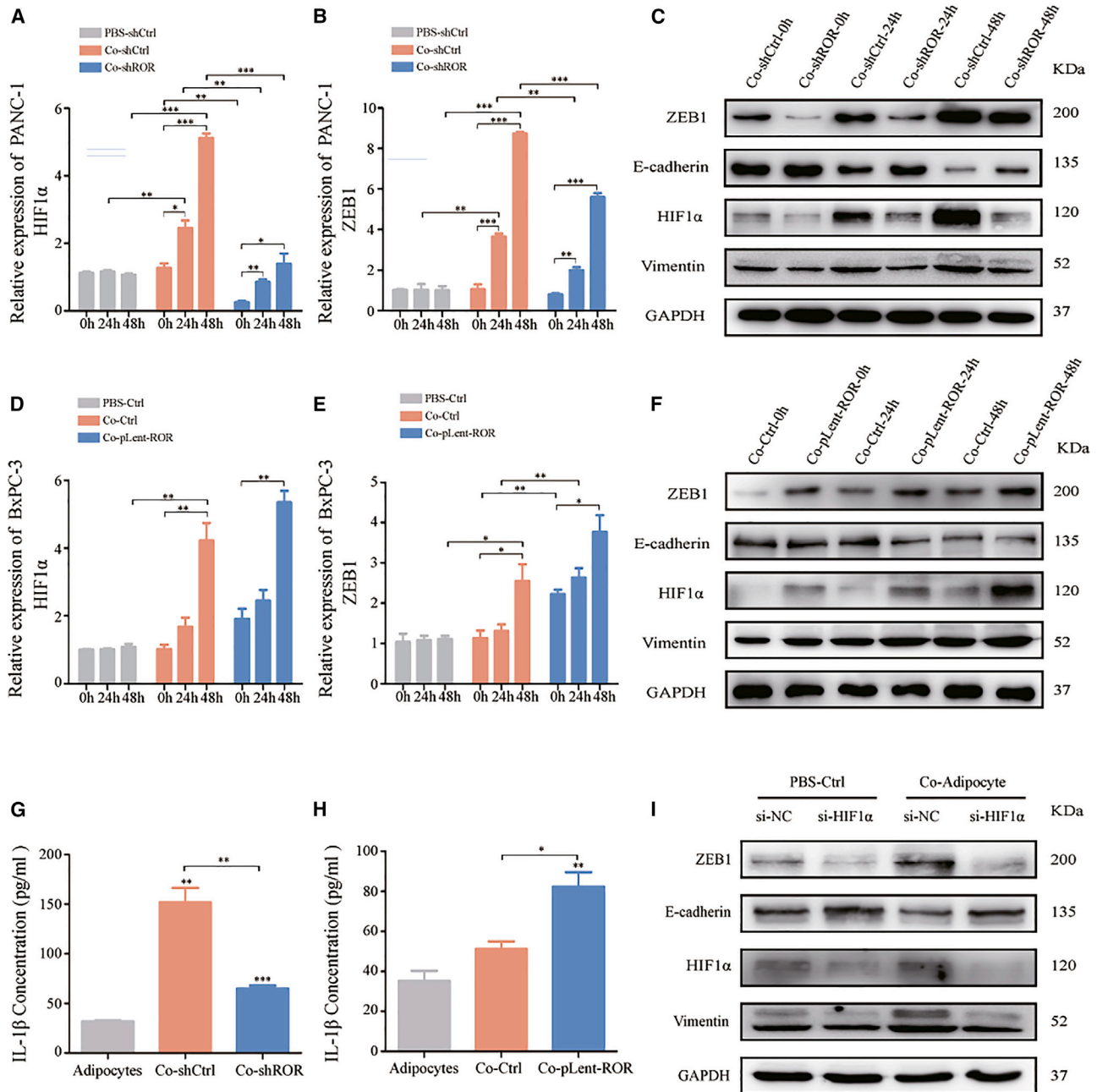
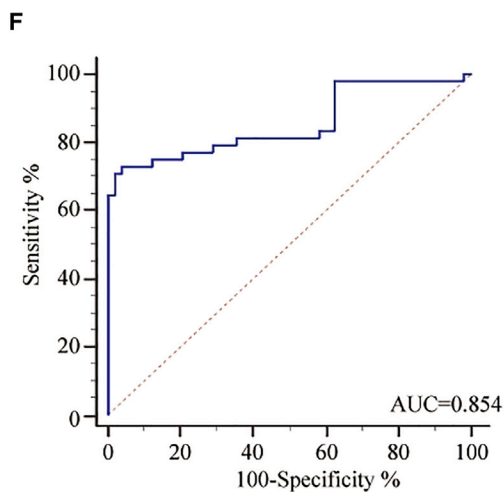
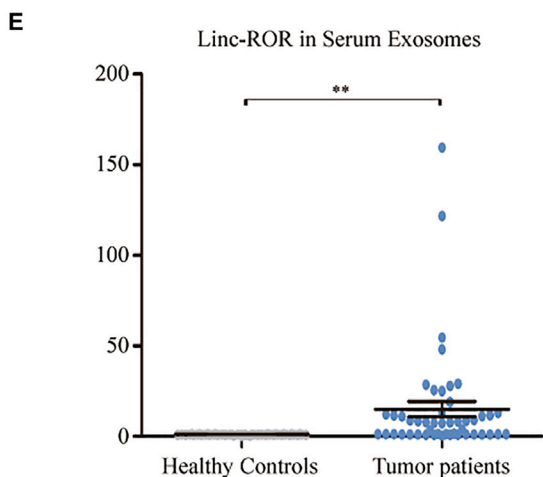
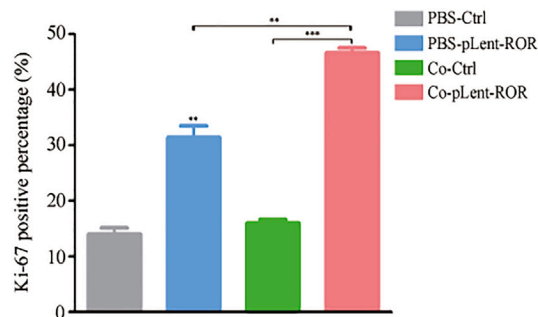
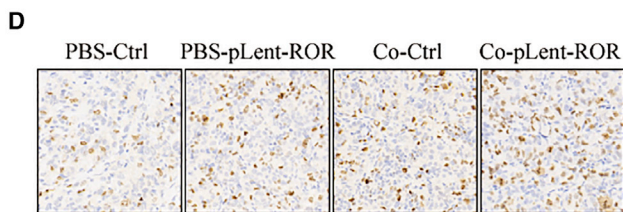
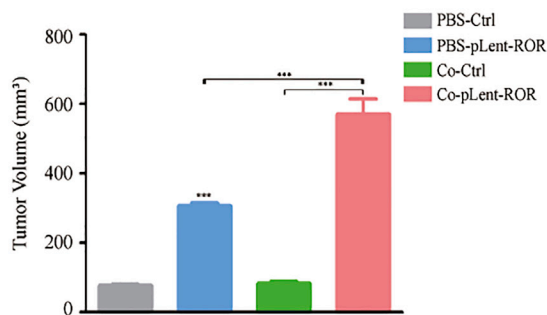
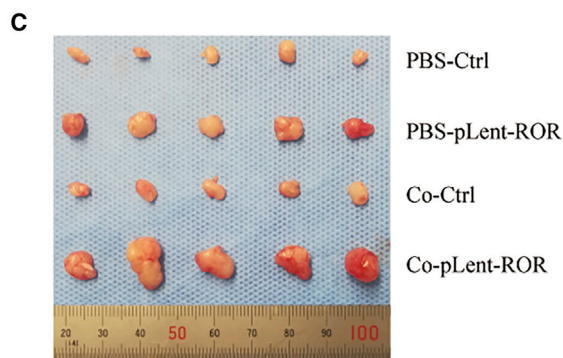
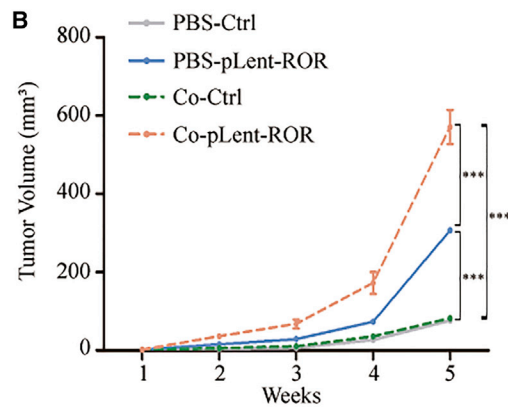
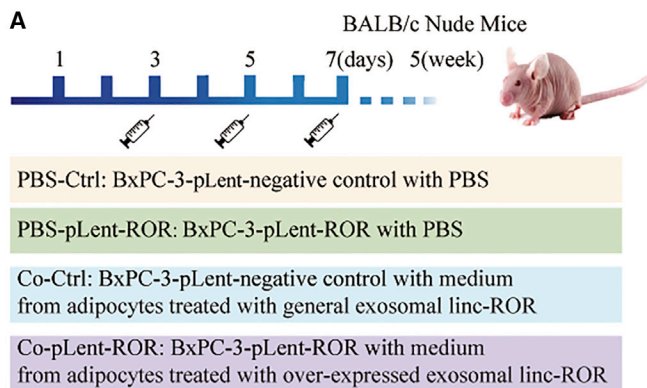


Figure 6. Exosomal linc-ROR induces dedifferentiation of adipocytes to facilitate EMT in PC cells by activating the HIF1 α -ZEB1 signaling pathway and increasing IL-1 β

(A and B) Quantitative real-time PCR assay was performed to detect linc-ROR expression and HIF1 α -ZEB1 expression in PANC-1 cells transfected with shCtrl and shROR in PBS (PBS-shCtrl) and coculture (CoshCtrl and CoshROR) systems for 0 h, 24 h, and 48 h. (D and E) Quantitative real-time PCR assay was performed to detect linc-ROR expression and HIF1 α -ZEB1 expression in BxPC-3 cells transfected with Ctrl and pLent-ROR in PBS (PBS-Ctrl) and coculture (Co-Ctrl and CopLent-ROR) systems for 0 h, 24 h, and 48 h. (C) Western blot analysis of E-cadherin, vimentin, HIF1 α , and ZEB1 protein expression in PANC-1 cells treated with CoshCtrl and CoshROR for 0 h, 24 h, and 48 h. (F) Western blot analysis of E-cadherin, vimentin, HIF1 α , and ZEB1 protein expression in BxPC-3 cells treated with Co-Ctrl and CopLent-ROR for 0 h, 24 h, and 48 h. (G and H) Expression of the cytokine IL-1 β in the supernatants of adipocytes cocultured with shCtrl-PANC-1 and shROR-PANC-1 cells compared to noncultured adipocytes. (I) PC cells transfected with HIF1 α siRNA (si-HIF1 α) or negative control siRNA (si-NC) were stimulated with or without conditioned medium from adipocytes, and protein expression of E-cadherin, vimentin, HIF1 α , and ZEB1 was determined.



(legend on next page)

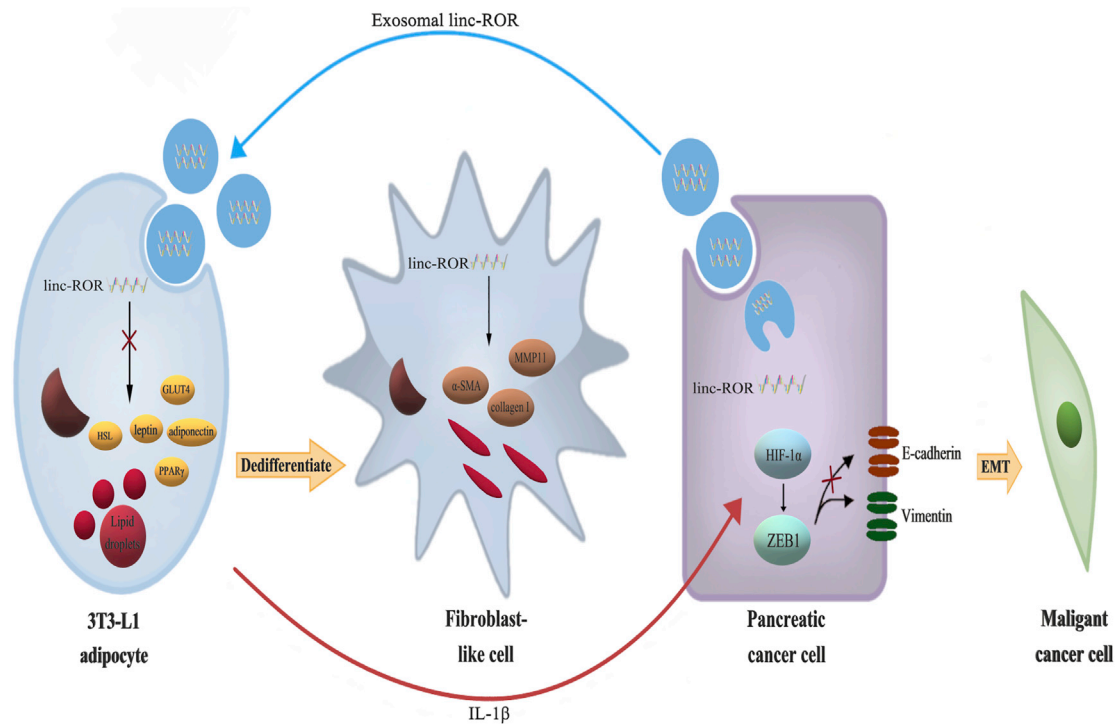


Figure 8. PC-cell-derived exosomal linc-ROR induces adipocytes to dedifferentiate into preadipocyte/fibroblast-like cells, which in turn sustain PC cell growth and invasion by activating the HIF1 α -ZEB1 signaling pathway through the cytokine IL-1 β .

primers, forward: 5'-GTCTTCACGTTGGTCTCGGT-3', reverse: 5'-CAGAGCCACGGTCATCAAGA-3'; HSL primers, forward: 5'-AGCCTCATGGACCCTCTCT-3', reverse: 5'-AGCGAAGTGTCTCTCTGCAC-3'; PPAR γ primers, forward: 5'-TGTCTCACAA TGCCATCAGGT-3', reverse: 5'-CAAATGCTTTGCCAGGGCTC-3'. Data processing was calculated by the ρ Ct method as described previously.⁵¹

Western blot analysis and ELISA assay

Western blotting was performed as previously reported.⁵¹ Antibodies used in the experiments were anti-CD9 (CST, #13403), anti-TSG101 (Abcam, #ab125011), anti-ZEB1 (CST, #3396), anti-HIF1 α (CST, #36169), anti-E-cadherin (CST, #3195), anti-vimentin (CST, #5741), anti-GLUT4 (CST, #2213), anti-PPAR γ (CST, #2435), anti-HSL (CST, #18381), anti- α -SMA (CST, #19245), anti-MMP11 (Invitrogen, #SN74-08), anti-collagen I (CST, #72026), and anti-GAPDH (CST, #5174). The mouse IL-1 β in culture medium was measured in the coculture or non-coculture experimental conditions using a Mouse IL-1 β ELISA Kit (Dakewe Biotech, #2012096).

IF assay

PC cells under different experimental conditions seeded on glass coverslips were fixed in 4% paraformaldehyde (PFA) for 30 min and then permeabilized with 0.25% Triton X-100 for 5 min. Each coverslip blocked with 4% bovine serum albumin was incubated with primary antibody against E-cadherin (CST, #3195) or vimentin (CST, #5741) for 4°C overnight, followed by the fluorescent secondary antibody at room temperature for 1 h. Cellular nuclei were stained using DAPI (Invitrogen). Images of the coverslips were observed under an Axio-Imager-LSM800 (ZEISS) as described previously.

Cell proliferation assay

After PC cells were seeded into 16-well plates, xCELLigence RTCA (ACEA Biosciences) was performed to examine cell growth ability to acquire real-time data for 96 h uninterruptedly. For plate clonality assays, a total of 1,000 PC cells with or without a coculture system were seeded into each well of a 6-well plate and maintained in medium at 37°C and 5% CO₂ for 2 weeks. Then, the number and size of colonies in each group were counted after the cells were stained

Figure 7. The tumor microenvironment mediated by exosomal linc-ROR facilitates tumor growth of PC cells via conditioned medium collected from adipocytes *in vivo*

(A) Experimental protocol of subcutaneous and intratumor injection of BALB/c nude mice. (B) Subcutaneous xenograft assay of BxPC-3 cells (5×10^6 cells) in nude mice with intratumor injection of PBS and conditioned medium from a coculture system. Tumor volumes of xenograft models were measured from day 0 to day 35. (C) Morphological characteristics of tumor xenografts formed by coinjection of different groups. (D) Expression of Ki-67 protein was examined by immunohistochemistry in xenograft tumor tissues. (E) RNA expression of exosomal linc-ROR was measured in the serum of healthy controls ($n = 48$) and the serum of PC patients ($n = 48$) using quantitative real-time PCR. (F) Receiver operator characteristic (ROC) curve for serum exosomal linc-ROR for the discrimination of patients with PC from normal healthy individuals.

with crystal violet (Beyotime). Cell proliferation was also measured by EdU assay (RiboBio) according to its specification in 96-well plates.

Cell-migration and wound-healing assays

The cell migration and invasion abilities of PC cells were evaluated using Transwell assays and wound-healing assays as previously described.⁵¹ All the above images were acquired using an inverted optical microscope (ZEISS).

Animal experiments

Male BALB/c nude mice (4 weeks old; Weitonglihua) were raised in a specific pathogen-free environment in the Animal Laboratory (the Second Hospital of Cheeloo College of Medicine, Shandong University). Twenty mice were randomly divided into four groups (5 mice per group). BxPC-3 cells (5×10^6 cells per mouse) mixed with or without conditioned medium from adipocytes stimulated with exosomes (linc-ROR overexpression or not) were injected into each nude mouse. Subsequently, intratumor injection of conditioned medium (three times a week) was performed. Tumor size and body weight were measured twice per week. After 5 weeks, all mice were sacrificed under general anesthesia after injection. Tumor tissues were prepared for histological examination by immunohistochemistry (IHC) of the Ki-67 protein. Immunohistochemistry assays were performed as previously reported.⁵² Tumor volume was calculated in mm^3 as $0.5 \times \text{width}^2 \times \text{length}$. All animal experiments were approved by the Institutional Animal Care and Use Committee and were performed according to the institution's guidelines and animal research principles.

Statistical analysis

SPSS 17.0 for Windows (IBM) and GraphPad Prism 6.0 (GraphPad Software) software were used for statistical analyses. Statistical evaluations were performed using Student's t test (two-tailed). The tumor marker diagnostic performance of exosomal linc-ROR was evaluated using MEDCALC 15.2.2 (Med-Calc). A p value of 0.05 or less was considered statistically significant. All results are expressed as the means \pm standard deviation (SD) of three independent experiments.

SUPPLEMENTAL INFORMATION

Supplemental information can be found online at <https://doi.org/10.1016/j.omtn.2021.06.001>.

ACKNOWLEDGMENTS

The authors thank Shandong Pancreatic Cancer Research Club (SPCRC) members for their suggestions and critiques to the manuscript. This work was supported by the National Natural Science Foundation of China (81702365 and 81972274), the Shandong Provincial Natural Science Foundation, China (ZR2017MH090), the Clinical Research Foundation of Shandong University (2020SDUCRCC016), and the Taishan Scholars Program of Shandong Province (tsqn202103172).

AUTHOR CONTRIBUTIONS

Z.W.S., D.S., L.T.D., Y.S.W., S.Y.H., and H.X.Z. contributed to the design of the study. Z.Y.F., J.Y., Y.Z.L., and Z.W.S. performed the experiments. Z.W.S., Y.J.F., B.Y.Z., P.S., and H.X.Z. contributed to the writing and revision of the manuscript. Z.W.S., D.S., B.Y.Z., L.T.D., Y.S.W., and H.X.Z. contributed to the material support of the study. All authors read and approved the final manuscript.

DECLARATION OF INTERESTS

The authors declare no competing interests.

REFERENCES

- Bray, F., Ferlay, J., Soerjomataram, I., Siegel, R.L., Torre, L.A., and Jemal, A. (2018). Global cancer statistics 2018: GLOBOCAN estimates of incidence and mortality worldwide for 36 cancers in 185 countries. *CA Cancer J. Clin.* 68, 394–424.
- Siegel, R.L., Miller, K.D., and Jemal, A. (2017). Cancer Statistics, 2017. *CA Cancer J. Clin.* 67, 7–30.
- Chen, W., Zheng, R., Baade, P.D., Zhang, S., Zeng, H., Bray, F., Jemal, A., Yu, X.Q., and He, J. (2016). Cancer statistics in China, 2015. *CA Cancer J. Clin.* 66, 115–132.
- Siegel, R.L., Miller, K.D., and Jemal, A. (2018). Cancer statistics, 2018. *CA Cancer J. Clin.* 68, 7–30.
- Stathis, A., and Moore, M.J. (2010). Advanced pancreatic carcinoma: current treatment and future challenges. *Nat. Rev. Clin. Oncol.* 7, 163–172.
- De La Cruz, M.S., Young, A.P., and Ruffin, M.T. (2014). Diagnosis and management of pancreatic cancer. *Am. Fam. Physician* 89, 626–632.
- Mohammed, S., Van Buren, G., 2nd, and Fisher, W.E. (2014). Pancreatic cancer: advances in treatment. *World J. Gastroenterol.* 20, 9354–9360.
- Ackerman, D., and Simon, M.C. (2014). Hypoxia, lipids, and cancer: surviving the harsh tumor microenvironment. *Trends Cell Biol.* 24, 472–478.
- Neesse, A., Algül, H., Tuveson, D.A., and Gress, T.M. (2015). Stromal biology and therapy in pancreatic cancer: a changing paradigm. *Gut* 64, 1476–1484.
- Zhan, H.X., Zhou, B., Cheng, Y.G., Xu, J.W., Wang, L., Zhang, G.Y., and Hu, S.Y. (2017). Crosstalk between stromal cells and cancer cells in pancreatic cancer: New insights into stromal biology. *Cancer Lett.* 392, 83–93.
- Davoodi, S.H., Malek-Shahabi, T., Malekshahi-Moghadam, A., Shahbazi, R., and Esmaeili, S. (2013). Obesity as an important risk factor for certain types of cancer. *Iran. J. Cancer Prev.* 6, 186–194.
- Berrington de Gonzalez, A., Sweetland, S., and Spencer, E. (2003). A meta-analysis of obesity and the risk of pancreatic cancer. *Br. J. Cancer* 89, 519–523.
- Incio, J., Liu, H., Suboj, P., Chin, S.M., Chen, I.X., Pinter, M., Ng, M.R., Nia, H.T., Grahovac, J., Kao, S., et al. (2016). Obesity-Induced Inflammation and Desmoplasia Promote Pancreatic Cancer Progression and Resistance to Chemotherapy. *Cancer Discov.* 6, 852–869.
- Kalra, H., Drummen, G.P., and Mathivanan, S. (2016). Focus on Extracellular Vesicles: Introducing the Next Small Big Thing. *Int. J. Mol. Sci.* 17, 170.
- Tkach, M., and Théry, C. (2016). Communication by Extracellular Vesicles: Where We Are and Where We Need to Go. *Cell* 164, 1226–1232.
- Kowal, J., Tkach, M., and Théry, C. (2014). Biogenesis and secretion of exosomes. *Curr. Opin. Cell Biol.* 29, 116–125.
- Xu, R., Greening, D.W., Zhu, H.J., Takahashi, N., and Simpson, R.J. (2016). Extracellular vesicle isolation and characterization: toward clinical application. *J. Clin. Invest.* 126, 1152–1162.
- Choi, D.S., Kim, D.K., Kim, Y.K., and Gho, Y.S. (2013). Proteomics, transcriptomics and lipidomics of exosomes and ectosomes. *Proteomics* 13, 1554–1571.
- Hewson, C., and Morris, K.V. (2016). Form and Function of Exosome-Associated Long Non-coding RNAs in Cancer. *Curr. Top. Microbiol. Immunol.* 394, 41–56.
- Zhan, H.X., Wang, Y., Li, C., Xu, J.W., Zhou, B., Zhu, J.K., Han, H.F., Wang, L., Wang, Y.S., and Hu, S.Y. (2016). LincRNA-ROR promotes invasion, metastasis and tumor

- growth in pancreatic cancer through activating ZEB1 pathway. *Cancer Lett.* 374, 261–271.
21. Wang, X., Luo, G., Zhang, K., Cao, J., Huang, C., Jiang, T., Liu, B., Su, L., and Qiu, Z. (2018). Hypoxic Tumor-Derived Exosomal miR-301a Mediates M2 Macrophage Polarization via PTEN/PI3K γ to Promote Pancreatic Cancer Metastasis. *Cancer Res.* 78, 4586–4598.
 22. Mincheva-Nilsson, L., and Baranov, V. (2014). Cancer exosomes and NKG2D receptor-ligand interactions: impairing NKG2D-mediated cytotoxicity and anti-tumour immune surveillance. *Semin. Cancer Biol.* 28, 24–30.
 23. Takahashi, K., Yan, I.K., Kogure, T., Haga, H., and Patel, T. (2014). Extracellular vesicle-mediated transfer of long non-coding RNA ROR modulates chemosensitivity in human hepatocellular cancer. *FEBS Open Bio* 4, 458–467.
 24. He, X., Yu, J., Xiong, L., Liu, Y., Fan, L., Li, Y., Chen, B., Chen, J., and Xu, X. (2019). Exosomes derived from liver cancer cells reprogram biological behaviors of LO2 cells by transferring Linc-ROR. *Gene* 719, 144044.
 25. Hardin, H., Helein, H., Meyer, K., Robertson, S., Zhang, R., Zhong, W., and Lloyd, R.V. (2018). Thyroid cancer stem-like cell exosomes: regulation of EMT via transfer of lncRNAs. *Lab. Invest.* 98, 1133–1142.
 26. Rákóczi, É., Perge, B., Végh, E., Csomor, P., Pusztai, A., Szamosi, S., Bodnár, N., Szántó, S., Szűcs, G., and Szekanez, Z. (2016). Evaluation of the immunogenicity of the 13-valent conjugated pneumococcal vaccine in rheumatoid arthritis patients treated with etanercept. *Joint Bone Spine* 83, 675–679.
 27. Maia, J., Caja, S., Strano Moraes, M.C., Couto, N., and Costa-Silva, B. (2018). Exosome-Based Cell-Cell Communication in the Tumor Microenvironment. *Front. Cell Dev. Biol.* 6, 18.
 28. Lu, X., and Kang, Y. (2010). Hypoxia and hypoxia-inducible factors: master regulators of metastasis. *Clin. Cancer Res.* 16, 5928–5935.
 29. Eltzschig, H.K., and Carmeliet, P. (2011). Hypoxia and inflammation. *N. Engl. J. Med.* 364, 656–665.
 30. Lee, J.W., Bae, S.H., Jeong, J.W., Kim, S.H., and Kim, K.W. (2004). Hypoxia-inducible factor (HIF-1 α): its protein stability and biological functions. *Exp. Mol. Med.* 36, 1–12.
 31. Joseph, J.V., Conroy, S., Pavlov, K., Sontakke, P., Tomar, T., Eggens-Meijer, E., Balasubramanian, V., Wagemakers, M., den Dunnen, W.F., and Kruyt, F.A. (2015). Hypoxia enhances migration and invasion in glioblastoma by promoting a mesenchymal shift mediated by the HIF1 α -ZEB1 axis. *Cancer Lett.* 359, 107–116.
 32. Werno, C., Menrad, H., Weigert, A., Dehne, N., Goerd, S., Schledzewski, K., Kzhyshkowska, J., and Brüne, B. (2010). Knockout of HIF-1 α in tumor-associated macrophages enhances M2 polarization and attenuates their pro-angiogenic responses. *Carcinogenesis* 31, 1863–1872.
 33. Fukumura, D., Incio, J., Shankarajah, R.C., and Jain, R.K. (2016). Obesity and Cancer: An Angiogenic and Inflammatory Link. *Microcirculation* 23, 191–206.
 34. Melo, S.A., Luecke, L.B., Kahlert, C., Fernandez, A.F., Gammon, S.T., Kaye, J., LeBleu, V.S., Mittendorf, E.A., Weitz, J., Rahbari, N., et al. (2015). Glypican-1 identifies cancer exosomes and detects early pancreatic cancer. *Nature* 523, 177–182.
 35. Allenson, K., Castillo, J., San Lucas, F.A., Scelo, G., Kim, D.U., Bernard, V., Davis, G., Kumar, T., Katz, M., Overman, M.J., et al. (2017). High prevalence of mutant KRAS in circulating exosome-derived DNA from early-stage pancreatic cancer patients. *Ann. Oncol.* 28, 741–747.
 36. Madhavan, B., Yue, S., Galli, U., Rana, S., Gross, W., Müller, M., Giese, N.A., Kalthoff, H., Becker, T., Büchler, M.W., and Zöller, M. (2015). Combined evaluation of a panel of protein and miRNA serum-exosome biomarkers for pancreatic cancer diagnosis increases sensitivity and specificity. *Int. J. Cancer* 136, 2616–2627.
 37. Deng, X., Ruan, H., Zhang, X., Xu, X., Zhu, Y., Peng, H., Zhang, X., Kong, F., and Guan, M. (2020). Long noncoding RNA CCAL transferred from fibroblasts by exosomes promotes chemoresistance of colorectal cancer cells. *Int. J. Cancer* 146, 1700–1716.
 38. Wang, D., Wang, X., Si, M., Yang, J., Sun, S., Wu, H., Cui, S., Qu, X., and Yu, X. (2020). Exosome-encapsulated miRNAs contribute to CXCL12/CXCR4-induced liver metastasis of colorectal cancer by enhancing M2 polarization of macrophages. *Cancer Lett.* 474, 36–52.
 39. Cui, R., Yue, W., Lattime, E.C., Stein, M.N., Xu, Q., and Tan, X.L. (2016). Targeting tumor-associated macrophages to combat pancreatic cancer. *Oncotarget* 7, 50735–50754.
 40. Nielsen, M.F., Mortensen, M.B., and Detlefsen, S. (2016). Key players in pancreatic cancer-stroma interaction: Cancer-associated fibroblasts, endothelial and inflammatory cells. *World J. Gastroenterol.* 22, 2678–2700.
 41. Zhou, B., Wu, D., Liu, H., Du, L.T., Wang, Y.S., Xu, J.W., Qui, F.B., Hu, S.Y., and Zhan, H.X. (2019). Obesity and pancreatic cancer: An update of epidemiological evidence and molecular mechanisms. *Pancreatology* 19, 941–950.
 42. Lee, Y., Jung, W.H., and Koo, J.S. (2015). Adipocytes can induce epithelial-mesenchymal transition in breast cancer cells. *Breast Cancer Res. Treat.* 153, 323–335.
 43. Kushiro, K., Chu, R.A., Verma, A., and Núñez, N.P. (2012). Adipocytes Promote B16BL6 Melanoma Cell Invasion and the Epithelial-to-Mesenchymal Transition. *Cancer Microenviron.* 5, 73–82.
 44. Lopez-Castejon, G., and Brough, D. (2011). Understanding the mechanism of IL-1 β secretion. *Cytokine Growth Factor Rev.* 22, 189–195.
 45. Tanaka, T., Narazaki, M., and Kishimoto, T. (2014). IL-6 in inflammation, immunity, and disease. *Cold Spring Harb. Perspect. Biol.* 6, a016295.
 46. Zhang, J., Zhang, Q., Lou, Y., Fu, Q., Chen, Q., Wei, T., Yang, J., Tang, J., Wang, J., Chen, Y., et al. (2018). Hypoxia-inducible factor-1 α /interleukin-1 β signaling enhances hepatoma epithelial-mesenchymal transition through macrophages in a hypoxic-inflammatory microenvironment. *Hepatology* 67, 1872–1889.
 47. Fu, X., Zhai, S., and Yuan, J. (2018). Interleukin-6 (IL-6) triggers the malignancy of hemangioma cells via activation of HIF-1 α /VEGFA signals. *Eur. J. Pharmacol.* 841, 82–89.
 48. Zhang, W., Shi, X., Peng, Y., Wu, M., Zhang, P., Xie, R., Wu, Y., Yan, Q., Liu, S., and Wang, J. (2015). HIF-1 α Promotes Epithelial-Mesenchymal Transition and Metastasis through Direct Regulation of ZEB1 in Colorectal Cancer. *PLoS ONE* 10, e0129603.
 49. Zhu, J., Huang, Z., Zhang, M., Wang, W., Liang, H., Zeng, J., Wu, K., Wang, X., Hsieh, J.T., Guo, P., and Fan, J. (2018). HIF-1 α promotes ZEB1 expression and EMT in a human bladder cancer lung metastasis animal model. *Oncol. Lett.* 15, 3482–3489.
 50. Théry, C., Amigorena, S., Raposo, G., and Clayton, A. (2006). Isolation and characterization of exosomes from cell culture supernatants and biological fluids. *Curr. Protoc. Cell Biol.* Chapter 3: Unit 3.22.
 51. Zhan, Y., Du, L., Wang, L., Jiang, X., Zhang, S., Li, J., Yan, K., Duan, W., Zhao, Y., Wang, L., et al. (2018). Expression signatures of exosomal long non-coding RNAs in urine serve as novel non-invasive biomarkers for diagnosis and recurrence prediction of bladder cancer. *Mol. Cancer* 17, 142.
 52. Qu, L., Ding, J., Chen, C., Wu, Z.J., Liu, B., Gao, Y., Chen, W., Liu, F., Sun, W., Li, X.F., et al. (2016). Exosome-Transmitted lncARSR Promotes Sunitinib Resistance in Renal Cancer by Acting as a Competing Endogenous RNA. *Cancer Cell* 29, 653–668.